

Published in final edited form as:

Cell Signal. 2011 September ; 23(9): 1489–1495. doi:10.1016/j.cellsig.2011.05.002.

Identification of new Gβγ interaction sites in adenylyl cyclase 2

Aislyn D.W. Boran¹, Yibang Chen¹, and Ravi Iyengar^{1,*}

¹Department of Pharmacology and Systems Therapeutics, Mount Sinai School of Medicine, One Gustave L. Levy Place, New York, NY 10029 USA

Abstract

The role of Gβγ in adenylyl cyclase (AC) signaling is complicated due to its role as a conditional activator (AC2, AC4 and AC7) and an inhibitor (AC1, AC3 and AC8). AC2 is stimulated by Gα_s and if Gβγ is present the stimulation is synergistic. The precise mechanism of this synergistic activation is still not known. In order to further elucidate the role of Gβγ in AC2 activation by Gα_s, peptides derived from the C1 domains of AC2 were synthesized and the ability of the various peptides to regulate AC2 function was tested. Our results identify two new Gβγ-binding sites in the AC2 C1 domain, AC2 C1a 339-360 and AC2 C1b 578-602 that are involved with stimulation of AC2 by Gβγ. These two regions are different from the previously described QEHA motif in the C2 domain of AC2. Further, the recently discovered PFAHL motif was confirmed to bind and to be involved with stimulation of AC2 by Gβγ. These functional studies indicate that multiple regions of AC2 are involved in the interaction with Gβγ.

Keywords

adenylyl cyclase; cyclic AMP; G-protein; Gβγ; Gα_s; peptide

1. Introduction

The adenylyl cyclases (AC 1-9) are the membrane-bound enzymes responsible for the generation of cAMP [1, 2]. The cAMP pathway orchestrates the signal transduction initiated by many hormones, neurotransmitters, and autocrine and paracrine factors to regulate a diversity of cellular functions [3]. Although the cAMP pathway is ubiquitous, both the receptors that couple to it and the various isoforms of the membrane-bound adenylyl cyclases that produce cAMP, are expressed in a tissue-selective manner [1]. Adenylyl cyclases are activated by stimulation of a variety of receptors coupled through the alpha unit (Gα_s) of the heterotrimeric guanine nucleotide binding protein, G_s. The various AC isoforms are also regulated by other molecules, such as calcium, calcium-calmodulin, calcium-calciuretin, cAMP dependent kinase, other G protein α-subunits (Gα_i, Gα_o and Gα_z) and Gβγ [4, 5]. Whether the regulatory interaction is stimulatory or inhibitory depends on the isoform of AC and the identity of the regulatory molecule. Gβγ activates AC2, AC4, and AC7 [6-12] in the presence of Gα_s or forskolin but inhibits AC1, AC3 and AC8 [12-15]. Gβγ interacts with AC5 and AC6 but whether the interaction is inhibitory or stimulatory is currently not clear [16, 17].

© 2011 Elsevier Inc. All rights reserved.

*To whom correspondence should be addressed: Phone: 212-659-1700 Fax: 212-831-0114 ravi.iyengar@mssm.edu .

Publisher's Disclaimer: This is a PDF file of an unedited manuscript that has been accepted for publication. As a service to our customers we are providing this early version of the manuscript. The manuscript will undergo copyediting, typesetting, and review of the resulting proof before it is published in its final citable form. Please note that during the production process errors may be discovered which could affect the content, and all legal disclaimers that apply to the journal pertain.

The interaction underlying the synergistic activation of AC2 by $G\beta\gamma$ in the presence of $G\alpha_s$ is the focus of this study. The AC2 site responsible for activation by $G\beta\gamma$ was tentatively assigned to the C-terminal half of the molecule [8]. Subsequently, a $G\beta\gamma$ -binding element, QEHA (QEHAQEPERQYMHIGTMVEFAYALVGK) on the C2a domain of AC2 was identified [9, 18]. Recently, it was discovered that while the QEHA motif in the C2a domain of AC2 was important for interaction with $G\beta\gamma$, a region coined the PFAHL motif (MTRYLESWGAAKPFAHL), in the C1b domain of AC2 was found to be essential for stimulation by $G\beta\gamma$ [15, 19]. Another recent study defined a region in the AC2 C2a domain, coined the KF-loop (LSKPKFSGV), as an essential motif for stimulation of $G\alpha_s$ activation AC2 by $G\beta\gamma$ [20]. Currently, it is not clear if these are the only regions involved in the interaction with AC2 or if other regions are involved.

In the present study, peptides derived from the C1a and C1b domains of AC2 were synthesized and the ability of the various peptides to bind to $G\beta\gamma$ and to inhibit AC2 activation by $G\beta\gamma$ was tested. Our results identify two new $G\beta\gamma$ -binding sites in the AC2 C1b domain. A peptide containing the sequence of the previously described [15] PFAHL motif was also confirmed to bind $G\beta\gamma$ and inhibit the stimulation of AC2 by $G\beta\gamma$.

2. Materials and Methods

2.1 Peptide synthesis

Peptides were either synthesized in-house or purchased from Celtek Peptides, Inc. (Nashville, TN). In-house synthesized peptides followed the Fmoc protocol on Wang resin. Fmoc-protected amino acids, Wang resin and HBTU (O-Benzotriazole-N,N',N'-tetramethyl-uronium-hexafluoro-phosphate) were purchased from Protein Technologies (Louisville, KY). The peptides were synthesized on a Symphony (Protein Technologies, Tucson, AZ) peptide synthesizer using the Fmoc protocol on Wang resin. Briefly, the resin was equilibrated in DMF (Fisher Scientific). Fmoc deprotection was achieved using piperidine (Sigma-Aldrich, St. Louis, MO) in N-methylmorpholine (NMP; Fisher Scientific). Coupling reactions were performed with 5-fold excess amino acid with respect to resin loading, in NMP with HBTU as a coupling reagent. The deprotection mixture consisted of trifluoroacetic acid (TFA), phenol, ethanedithiol, thioanisole and H_2O (ratio of 10:0.75:0.25:0.50:0.50; all from Sigma-Aldrich). Peptides were extracted with ether and dried under nitrogen. The purity of the peptides was assessed by HPLC on a C_{18} reversed phase (RP) column (Grace-Vydac, Columbia, MD) with solvent A as 0.1% TFA in H_2O and solvent B as 0.1% TFA in acetonitrile and on a gradient of 0.5% B per min. If peptides were less than 80% pure, purification was performed using a semi-preparative C_{18} RP column. Masses were verified by MALDI-TOF (Voyager-DE PRO MALDI-TOF, Applied Biosystems, Foster City, CA) at the Mass Spectrometry Core Facility, Weill Medical College of Cornell University in New York, NY.

2.2 Biacore surface plasmon resonance binding assays

All experiments were performed on a Biacore 2000 instrument. Biotinylated peptides were immobilized on a streptavidin Biacore chip. A solution of $G\beta\gamma$ in 25 mM HEPES (pH 8.0) was flowed over each chip at concentrations of 12.5, 25, 50, 100 and 200 nM, at a flow rate of 20 $\mu L/min$. The data were fitted using the Biacore Biaevaluation software (Version 3.1) to determine the K_D value for each peptide. The residue plots represent the efficiency of data-fitting at each timepoint in the binding isotherm.

2.3 Adenylyl cyclase activity assays

Two assay types were used to assess AC2 activity in membrane preparations from Hi5 cells infected with recombinant AC2 baculovirus. The membrane preparation was described

previously [21]. The constitutively active form of $G\alpha_s$ (Q227L) was synthesized as described by Harry et al. [22]. $G\beta\gamma$ was isolated from Hi5 cells using the protocol previously described protocol [23]. Baculovirus constructs for $G\beta 1$ and His-tagged $G\gamma 2$ were kindly provided by Jim Garrison (Department of Pharmacology, University of Virginia).

The radioactive activity assay for detection of [α - ^{32}P]ATP conversion to [^{32}P]cAMP has been described [22, 24]. Briefly, the peptides were mixed with adenylyl cyclase-expressing membranes and held on ice for 10 min prior to assays. AC2-membranes were added to assay tubes such that the final amount of membrane protein per tube was 1–2 μg . The concentration of activated $G\alpha_s$ was 2 nM and that of $G\beta\gamma$ was 200 nM. The ability of the peptide to inhibit $G\alpha_s$ activation of AC2 and basal AC2 activity was also tested.

The non-radioactive cAMP assay kit (Lance cAMP assay) was purchased from Perkin Elmer Life and Analytical Sciences (Wellesley, MA). The manufacturer's protocol was followed with the exception of using a membrane preparation (1 μg of AC2 membrane protein per well) in place of cells. The stimulation buffer contained 20 mM Hepes pH 8.0, 2 mM DTT, 1 mM EDTA, 11 mM MgCl_2 , 100 μM ATP with regeneration system (myokinase, creatine phosphokinase and creatine phosphate) and a mixture of protease inhibitors (0.5 mM IBMX, 3.2 $\mu\text{g}/\text{ml}$ leupeptin, 1 $\mu\text{g}/\text{ml}$ aprotinin, 1 mM phenanthroline, and 1 mM phenylmethylsulfonyl fluoride). The peptides were dissolved in stimulation buffer at 4 times the assay concentration. Next, 5 μL of the peptide solutions were pipetted to the assay plate (Costar, 96-well half-area, white-walled) followed by 5 μL $G\alpha_s$ and $G\beta\gamma$ at double the assay concentration. The solution of peptide with G proteins was incubated for 30 minutes at room temperature. Next, 10 μL of the AC2 membranes (2 μg membrane protein per well) in stimulation buffer was added and the stimulation reaction was incubated for 15 minutes at room temperature. The final concentrations of $G\alpha_s$ and $G\beta\gamma$ were 20 nM and 1 μM , respectively. Controls for basal cAMP level, $G\alpha_s$ -stimulation alone and $G\alpha_s$ + $G\beta\gamma$ -stimulation without peptide are run alongside peptide samples. Samples were read using a Wallac Envision 2101 Multilabel Reader with Wallac Envision Manager software and the manufacturer's recommended settings. A standard curved was generated using a standardized cAMP solution diluted in stimulation buffer and the Lance fluorescence values are converted to cAMP concentrations by interpolating the values using a non-linear regression in GraphPad Prism Version 5.

All experiments were repeated two or more times with qualitatively similar results. Typical experiments are shown. Values are means of duplicate determinations and coefficients of variance were < 7%.

3. Results

3.1 Peptide design and synthesis

Several peptides with sequences of regions the C1 domain of AC2 were synthesized (Figure 1). The sequences were designed to cover regions the C1b domain almost in its entirety and a region from the C1a domain that displays high homology, specifically higher amongst the adenylyl cyclase isoforms stimulated by $G\beta\gamma$ (Figure 7A) than in the AC isoforms that are stimulated by $G\beta\gamma$ (AC2, AC4, AC5, AC6 and AC7). The relative location of the peptides in the AC2 sequence is depicted by color-coding in the AC2 structural schematic (Figure 1A) and their sequences are displayed (Figure 1B). We originally synthesized the AC2 C1b 495-514 peptide (RYLESWGAAKPFAHLHHRDS) that differed by several residues from the published PFAHL region analyzed by Diel et al. (493-509, MTRYLESWGAAKPFAHL) [15]. For direct comparison, we synthesized the PFAHL region peptide (AC2 C1b 493-509) used by Diel et al. [15]. We also synthesized a peptide

from the region adjacent to the PFAHL sequence, AC2 C1b 514-541. Data for the previously published QEHA region (AC2 C2 956-982) is shown for comparison.

3.2 Several novel regions of AC2 display a binding interaction with G $\beta\gamma$

Biacore surface plasmon resonance (SPR) was used to determine the binding affinity of the peptides for G $\beta\gamma$ by flowing varying concentrations of G $\beta\gamma$ over the biotin-immobilized peptide surface. Several peptides with sequences within the AC2 C1a, C1b and C2 regions displayed high affinities for G $\beta\gamma$ (Table 1). The QEHA region peptide (C2 956-982), previously reported to interact with G $\beta\gamma$ [25], displayed a K_D of 13.9 ± 8.8 nM (Figure 4D, Table 1). A new, C1a region (339-360, CY YCVSGLPISLPNHAKNCVKM), was found to bind G $\beta\gamma$ (K_D 40.5 ± 6.3 nM, Figure 2A, Table 1). Peptides which encode the C1b region in entirety were tested and the PFAHL region peptides and a novel region (578-602, ISLLFYNKVLEKEYRATALPAFKYY) were found to have a high affinity interaction with G $\beta\gamma$ (Table 1). AC2 C1b 578-602 had a K_D of 102 ± 14 nM (Figure 4B). The PFAHL peptides had similar affinities AC2 C1b 493-509 (K_D 2.7 ± 1.3 nM, Figure 3A) and 495-514 (K_D 2.7 ± 1.3 nM, Figure 3B). The other C1b peptides tested, 515-541 (MTTENGKISTTDVPMGQHNFQNRTLR) and 554-577 (ERMIQAIDGINAQKQWLKSEDIQR) displayed minimal affinity ($K_D > 10$ μ M) (Figure 3C and 4A). To rule out non-specific binding, several amino acids were changed to alanines and charged amino acids were changed to oppositely charged amino acids in the C1a and one C1b high affinity peptides (AC2 C1a 339-360 scrm and AC2 C1b 578-602 scrm, Figure 1B). The scrambled forms of the C1a 339-360 and C1b 578-602 peptides did not display affinity for G $\beta\gamma$ (Table 1 and Figure 2B and Figure 4C, respectively).

3.3 Several new regions of AC2 mediate synergistic stimulation by G α_s and G $\beta\gamma$

The ability of the various peptides to reduce the stimulation of AC2 by G $\beta\gamma$ and G α_s was assayed. G α_s increases the activity of AC2 by approximately 2- to 5-fold over basal and G $\beta\gamma$ further increases G α_s – stimulated AC2 activity another 3- to 6-fold (15- to 30-fold over basal, Figures 5 and 6). The C1a (339-360), C1b (578-602), C1b (495-514) and C1b (493-509) peptides inhibited G α_s /G $\beta\gamma$ stimulation of AC2. The 578-602 C1b peptide inhibited G $\beta\gamma$ stimulation of G α_s -activated AC2 completely, bringing the cAMP level below that of G α_s stimulation (Figure 5A) with an IC_{50} of 578-602 of 2.2 μ M (Table 2). The C1a (339-360) exhibited a strong inhibition of G $\beta\gamma$ stimulation of G α_s -activated AC2 (Figure 5A), with an inhibition of 88.0% at the highest concentration tested (300 μ M) and IC_{50} of 5.6 μ M peptide (Table 2). The PFAHL C1b (493-509 and 495-514) peptides exhibited inhibition of G $\beta\gamma$ synergistic stimulation of AC2 (Figure 5A and 6A) with the 495-514 peptide displaying 67.0% maximal inhibition with an IC_{50} value of 13.9 μ M (Table 2). The C1b peptides that did not display binding to G $\beta\gamma$ in the Biacore SPR assay (C1b 515-541, 554-577), also did not display any inhibitory effect in G $\beta\gamma$ activation of AC2. With the exception of the 578-602 C1b peptide, all of peptides exhibited a partial inhibition on G α_s activity alone at higher concentrations of peptide (Figure 5B and 6B). The maximal inhibitions of G α_s active ranged from 15.3 to 39.1% and the IC_{50} values ranged from 36.7 to 82.3 μ M (Table 2). The 578-602 C1b peptide, exhibited a more pronounced effect (Figure 5B and 6B). The maximal inhibition by the 578-602 C1b peptide on G α_s activity was 50.6%, with an IC_{50} value of 2.5 μ M (Table 2). All of the peptides caused a small reduction of basal activity (maximal 14.1 to 36.7%) with IC_{50} values ranging from 7.7 to >100 μ M (Table 2 and Figures 5C and 6C).

4. Discussion

Depending on the identity of adenylyl cyclase isoform, G $\beta\gamma$ either activates or inhibits the enzyme. Specifically, AC2, AC4, and AC7 [6-12] are activated by G $\beta\gamma$ in the presence of

$G\alpha_s$ or forskolin and AC1, AC3 and AC8 [12-15] are inhibited by $G\beta\gamma$. AC5 and AC6 interact with $G\beta\gamma$ but whether the interaction is inhibitory or stimulatory is yet to be determined [16, 17]. There is prominent homology (77-90%) between AC2, AC4 and AC7 in the C1b AC2 region, which also markedly changes amongst the AC isoforms that are inhibited by $G\beta\gamma$ (AC1, AC3, AC5, AC6 and AC8) (Figure 7B). There is also homology within a section of the C1a region of AC2 (Figure 7A). Therefore, a series of peptides representing the highly homologous AC2 C1b and AC2 C1a regions and a previously identified AC2 C2 region were synthesized and assayed (Figure 1). Binding between immobilized AC2 peptides and $G\beta\gamma$ was tested using Biacore SPR. The ability of the AC2 peptides to inhibit $G\beta\gamma$ -mediated synergistic activation of $G\alpha_s$ -induced AC2 activity was assayed.

The $G\beta\gamma$ -interaction of the previously identified AC2 C2 QEHA peptide was confirmed using Biacore SPR, along with the $G\beta\gamma$ -interaction of the AC2 C1b PFAHL region (Figures 4D, 3A and 3B and Table 1). Two AC2 peptides bound to $G\beta\gamma$ with affinities in the nanomolar range, representing two new interactions of $G\beta\gamma$ within the C1a region (AC2 C1a 339-360) and C1b region of AC2 (AC2 C1b 578-602; Figures 2A and 4B and Table 1). Two other C1b region peptides did not interact with $G\beta\gamma$ (AC2 C1b 515-541 and 554-577; Figures 3C and 4A and Table 1). Control, scrambled peptides (AC2 C1a 339-360 scrm and AC2 C1b 578-602 scrm) did not interact with $G\beta\gamma$, indicating that the detected binding was specific (Figures 2B and 4C and Table 1).

Two new regions of AC2 which interacted with $G\beta\gamma$ by Biacore SPR were shown to be involved with the activation of $G\alpha_s$ -stimulated AC2 by $G\beta\gamma$ using an enzymatic activity assay. The C1a 339-360 peptide domain almost completely inhibited $G\alpha_s$ / $G\beta\gamma$ -mediated AC activation (Figure 5A and Table 2), with minimal effect on $G\alpha_s$ -mediated activity alone (Figure 5B and Table 2). The AC2 C1b 578-602 peptide most strongly inhibited $G\alpha_s$ / $G\beta\gamma$ -mediated AC2 activation (Figure 5A and Table 2), but also partially inhibited $G\alpha_s$ -mediated activation of AC2. As shown previously by Diel et al. [15], the PFAHL peptides, AC2 C1b inhibited activation of AC2 by $G\beta\gamma$ in the presence of $G\alpha_s$ (Figures 5A and 6A and Table 2). The two C1b peptides from the AC2 C1b region which lacked homology, AC2 515-541 and 554-577, did not have an effect on the synergistic $G\alpha_s$ / $G\beta\gamma$ -stimulation of AC2 (Figure 5A and Table 2). The C1b peptide 542-553 was not assayed due to synthesis difficulties.

Our Biacore findings indicate that the binding affinities of the interacting peptides from AC2 have increasing affinity for $G\beta\gamma$ in the following order: C1b 578-602 (102 nM), C1a 339-360 (40.5 nM), QEHA (13.9 nM), and C1b PFAHL or 495-514 (2.7 to 4.7 nM). The abilities to block $G\alpha_s$ / $G\beta\gamma$ -mediated activation of AC2 of the interacting peptides increase as follows, according to their maximal inhibition of AC2: C1b PFAHL 495-514 (67.0%), C1a 339-360 (88.0%) and C1b 578-602 (>100%). The trends of the binding and activity differ, but the inhibition of $G\alpha_s$ -activity alone must be taken into account. The C1b 578-602 peptide bound with the weakest affinity and showed the strongest inhibition of $G\beta\gamma$ / $G\alpha_s$ activity, but also inhibited $G\alpha_s$ activity alone the most strongly, by 50.6%. The relatively low affinity of and relatively strong inhibition of $G\alpha_s$ activity by the C1b 578-602 peptide supports the possibility that this C1b sequence spans the two regions of AC2 that interact with $G\beta\gamma$ and $G\alpha_s$. Alternatively, this peptide may cause a rearrangement of AC2 which allosterically affects $G\alpha_s$ -mediated AC2 activity. The PFAHL peptide(s) bound to $G\beta\gamma$ with the highest affinity and showed the weakest relative inhibition of $G\beta\gamma$ / $G\alpha_s$ activity, but this peptide had a minimal effect on $G\alpha_s$ activity alone, indicating that this region of AC2 mediates the $G\beta\gamma$ interaction alone. The C1a region has an affinity of 40 nM, in the middle trend of the AC2 interacting regions, and this peptide inhibited $G\beta\gamma$ / $G\alpha_s$ activity by 88% with 36.1% inhibition of $G\alpha_s$ activity alone only at higher concentrations (IC_{50} of 82.3 μ M). This result supports the possibility that this novel C1a region also interacts with $G\beta\gamma$ alone.

The binding and activity data are supported by the homology across the AC isoforms in each region. The strong homology between AC2, AC4, and AC7 in the C1a 339-360 region (85%) and PFAHL region (80-89%) corroborates that these regions are functionally important for the interaction of $G\beta\gamma$ with the AC isoforms that are $G\beta\gamma$ -stimulated (Figure 7A and 7B). The homology in this region is present in the C1a region of the AC isoforms that are inhibited by $G\beta\gamma$ (AC1, AC3, AC5, AC6 and AC8), albeit to a lesser extent (51-65%), indicating that this region may play a role in the inhibitory $G\beta\gamma$ mechanism as well (Figure 7A). The homology in the PFAHL region markedly decreases (10-26%) amongst the AC isoforms that are inhibited by $G\beta\gamma$ (AC1, AC3, AC5, AC6 and AC8) (Figure 7B), indicating that this region most likely does not play a role in the inhibitory $G\beta\gamma$ mechanism. There is strong homology (60%) between AC2 and AC4 in the 578-602 C1b AC2 region (Figure 7B), which is reduced to 32% in AC7. The reduction in homology indicates that the mechanism of $G\beta\gamma$ -activation of the AC2 and AC7 may differ slightly with respect to this region being less important for AC7 activation. The homology in the 578-602 region markedly decreases amongst most AC isoforms that are inhibited by $G\beta\gamma$ (28-32% homology for AC5, AC6 and AC8 and 12% homology for AC1 and AC3, Figure 7B). The C1b region from 515-577 displays negligible homology across all the AC isoforms and the peptides from these regions did not display binding or strong inhibition of AC2 activity.

Structural [27] and activity data [24, 28] support that the C1 and C2 domains of AC are brought together by $G\alpha_s$ to allosterically activate the enzyme. The available AC structure was determined using AC5 C1 (residues 364-580) and ACII C2 (residues 874-1081) and only partially encompasses the cytosolic domains [27]. The AC constructs have a relatively low affinity for one another and minimal activity; however, in the presence of $G\alpha_s$ a high-affinity, active ($\geq 150 \mu\text{mol/min/mg}$) complex is formed [28], supporting the notion that $G\alpha_s$ brings the two domains together in an active formation. We propose that during this structural reorganization, the $G\beta\gamma$ -binding face on AC2 becomes exposed. Including the data reported herein, there are now five reported areas within AC2 that interact with $G\beta\gamma$: one within the C1a region (339-360, reported here), two within the C1b region (PFAHL reported previously [15] and here and 578-602 reported here) and two within the C2 region (KF loop 925-933 reported previously [20] and QEHA reported by us and others [9, 18, 19, 29] and confirmed here). Taken together, these data support that $G\beta\gamma$ binds to several areas both the C1 and C2 regions of AC and that $G\beta\gamma$ allosterically rearranges the domains to a position that further favors enzymatic activity.

The structure of AC in complex with $G\alpha_s$ [27, 30] is displayed in Figure 7C, with AC5 C1 shown in green and AC2 C2 shown in red and $G\alpha_s$ is shown in blue. The structure of the AC C1b domain has not been solved and is represented by a dashed circle at the C-terminal region of the C1a domain in Figure 7C. Of the regions that are present in the structure, the $G\alpha_s$ -interaction regions within AC are non-overlapping with the $G\beta\gamma$ -interaction regions. The regions of AC2 that interact with $G\alpha_s$ include AC2 C2 $\alpha 2'$ region (904-921), AC2 C2 $\alpha 3'$ region (986-992) and the AC5 C1 N-terminal loop region (378-379). The AC2 $\alpha 3'$ region (986-992) region is proximal to but not overlapping with the QEHA region (956-982, highlighted in cyan in Figure 7C). The KF loop (927-933, highlighted in purple in Figure 7C) is proximal to the QEHA region and non-overlapping with $G\alpha_s$ -interaction regions. The C1a region (339-360, highlighted in orange in Figure 7C) is exposed in the $G\alpha_s$ -AC structure and includes a flexible loop region that most likely forms contacts with $G\beta\gamma$. The C1b regions (PFAHL 493-514 and 578-602) were not included in the AC construct used for crystallization [27]. However, since the included $G\beta\gamma$ -interaction regions are arranged on one face of AC2 which is proximal to the C-terminal of the C1a domain, it is likely that the C1b domain extends in such a way that the $G\beta\gamma$ -binding regions within C1b are accessible to $G\beta\gamma$ (Figure 7C).

In previous studies, we have shown that the Switch I and II regions of $G\alpha_s$ are important for stimulation of AC2 [24]. Due to the construct of AC crystallized for the structure, the Switch I-AC interaction is omitted. The Switch I and II regions of $G\alpha_s$ are also involved in interactions between $G\alpha_s$ and $G\beta\gamma$ [22]. Thus the areas of $G\alpha_s$ which have affinity for $G\beta\gamma$ are occluded when $G\alpha_s$ is bound to AC2. This supports the notion that $G\alpha_s$ initially binds to AC2, structurally rearranging AC2 to expose the $G\beta\gamma$ -binding face, which is mutually exclusive from the $G\alpha_s$ binding face.

In conclusion, we have identified two novel regions of AC2 which play a role in the synergistic activation by $G\beta\gamma$ of $G\alpha_s$ -stimulated AC2. Our data support that $G\beta\gamma$ binds to the C1b face of AC2 that is exposed upon $G\alpha_s$ binding and that $G\beta\gamma$ binding to AC2 further rearranges the AC2 active site in order to increase the rate of substrate turnover. In order to definitively establish that the rearrangement of AC2 by $G\alpha_s$ -binding exposes a $G\beta\gamma$ -binding surface, it is necessary to obtain structural data to allow for comparison of the bound and unbound structures. Currently no structural data of full-length, membrane-bound adenylyl cyclases are available. Even with the full structural data for AC2, the activation process is complex and there are most likely to be differences across AC isoforms. Thus, the definitive understanding of how $G\alpha_s$ and $G\beta\gamma$ activate adenylyl cyclase awaits advances in crystal structures of membrane bound proteins. Recent data have shown that different isoforms of AC play different roles in opiate induced AC superactivation or superinhibition and that $G\beta\gamma$ plays a critical role in this signal regulation [31-33]. Also, current data suggests a role for $G\beta\gamma$ dimers in these processes [34]. The mechanistic information revealed by this study contributes to the overall understanding of the complex signaling involved with adenylyl cyclases and $G\beta\gamma$.

Acknowledgments

This research is supported by NIH grant CK-38761 and GM54508.

References

- [1]. Iyengar R. FASEB J. 1993; 7:768–755. [PubMed: 8330684]
- [2]. Taussig R, Gilman AG. 1995; 270:1–4.
- [3]. Ross EM, Gilman AG. Annu. Rev. Biochem. 1980; 49(533-564)
- [4]. Tang WJ, Yan S, Drum CL. Adv. Second Messenger Phosphoprotein Res. 1998; 32:137–151. [PubMed: 9421589]
- [5]. Pieroni J, Jacobowitz O, Chen J, Iyengar R. Curr. Opin. Neurobiol. 1993; 3:345–351. [PubMed: 8369627]
- [6]. Gao X, Sadana R, Dessauer CW, Patel TB. J. Biol. Chem. 2007; 282(1):294–308. [PubMed: 17110384]
- [7]. Steiner D, Saya D, Schallmach E, Simonds WF, Vogel Z. Cell. Signal. 2006; 18(1):62–68. [PubMed: 15925485]
- [8]. Tang WJ, Gilman AG. Science. 1991; 254(5037):1500–1503. [PubMed: 1962211]
- [9]. Chen J, DeVivo M, Dingus J, Harry A, Li J, Sui J, Carty DJ, Blank JL, Exton JH, Stoffel RH, Inglese J, Lefkowitz RJ, Logothetis DE, Hildebrandt JD, Iyengar R. Science. 1995; 268(5214): 1166–1169. [PubMed: 7761832]
- [10]. Gao BN, Gilman AG. Proc. Natl. Acad. Sci. USA. 1991; 88(22):10178–10182. [PubMed: 1946437]
- [11]. Yoshimura M, Ikeda H, Tabakoff B. Mol Pharmacol. 1996; 50(4):43–51. [PubMed: 8700117]
- [12]. Choi E-J, Xia Z, Villacres EC, Storm DR. Curr. Opin. Cell Biol. 1993; 5(2):269–273. [PubMed: 8507499]
- [13]. Taussig R, Quarmby LM, Gilman AG. J Biol Chem. 1993; 268(1):9–12. [PubMed: 8416978]

- [14]. Tang W-J, Krupinski J, Gilman AG. J Biol Chem. 1991; 266(13):8595–8603. [PubMed: 2022671]
- [15]. Diel S, Klass K, Wittig B, Kleuss C. J. Biol. Chem. 2006; 281(1):288–294. [PubMed: 16275644]
- [16]. Gao X, Sadana R, Dessauer CW, Patel TB. J Biol Chem. 2007; 282(1):294–302. [PubMed: 17110384]
- [17]. Bayewitch ML, Avidor-Reiss T, Levy R, Pfeuffer T, Nevo I, Simonds WF, Vogel Z. FASEB J. 1998; 12(11):1019–1025. [PubMed: 9707174]
- [18]. Weng G, Li J, Dingus J, Hildebrandt JD, Weinstein H, Iyengar R. J Biol Chem. 1996; 271:26445–26448. [PubMed: 8900107]
- [19]. Weitmann S, Schultz G, Kleuss C. Biochemistry. 2001; 40(36):10853–10858. [PubMed: 11535062]
- [20]. Diel S, Beyermann M, Llorens JM, Wittig B, Kleuss C. Biochem J. 2008; 411(2):449–456. [PubMed: 18215138]
- [21]. Pieroni JP, Harry A, Chen J, Jacobowitz O, Magnusson RP, Iyengar R. J. Biol. Chem. 1995; 270(36):21368–21373. [PubMed: 7673172]
- [22]. Harry A, Chen Y, Magnusson R, Iyengar R, Weng G. J. Biol. Chem. 1997; 272(30):19017–19021. [PubMed: 9228084]
- [23]. Davis TL, Bonacci TM, Sprang SR, Smrcka AV. Biochemistry. 2005; 44(31):10593–10604. [PubMed: 16060668]
- [24]. Chen Y, Yoo B, Lee JB, Weng G, Iyengar R. J. Biol. Chem. 2001; 276:45751–45754. [PubMed: 11579096]
- [25]. Chen J, Bander JA, Santore TA, Chen Y, Ram PT, Smit MJ, Iyengar R. Proc. Natl. Acad. Sci. USA. 1998; 94:2648–2652. [PubMed: 9482941]
- [26]. Chen J, DeVivo M, Dingus J, Harry A, Li J, Sui J, Carty DJ, Blank JL, Exton JH, Stoffel RH, et al. Science. 1995; 268(5214):1166–1169. [PubMed: 7761832]
- [27]. Tesmer JJ, Sunahara RK, Gilman AG, Sprang SR. Science. 1997; 278(5345):1907–1916. [PubMed: 9417641]
- [28]. Sunahara RK, Dessauer CW, Whisnant RE, Kleuss C, Gilman AG. J Biol Chem. 1997; 272(35):22265–22271. [PubMed: 9268375]
- [29]. Chen Y, Weng G, Li J, Harry A, Pieroni J, Dingus J, Hildebrandt JD, Guarnieri F, Weinstein H, Iyengar R. Proc Natl Acad Sci U S A. 1997; 94(6):2711–2714. [PubMed: 9122261]
- [30]. Tesmer JJ, Sunahara RK, Johnson RA, Gosselin G, Gilman AG, Sprang SR. Science. 1999; 285(5428):756–760. [PubMed: 10427002]
- [31]. Avidor-Reiss T, Nevo I, Levy R, Pfeuffer T, Vogel Z. J Biol Chem. 1996; 271(35):21309–21315. [PubMed: 8702909]
- [32]. Avidor-Reiss T, Nevo I, Saya D, Bayewitch M, Vogel Z. J Biol Chem. 1997; 272(8):5040–5047. [PubMed: 9030567]
- [33]. Schallmach E, Steiner D, Vogel Z. Neuropharmacology. 2006; 20(8):998–1005. [PubMed: 16545401]
- [34]. Steiner D, Avidor-Reiss T, Schallmach E, Saya D, Vogel Z. J Mol Neurosci. 2005; 27(2):192–203.
- [35]. Pymol by DeLano Scientific LLC. <http://pymol.sourceforge.net/>

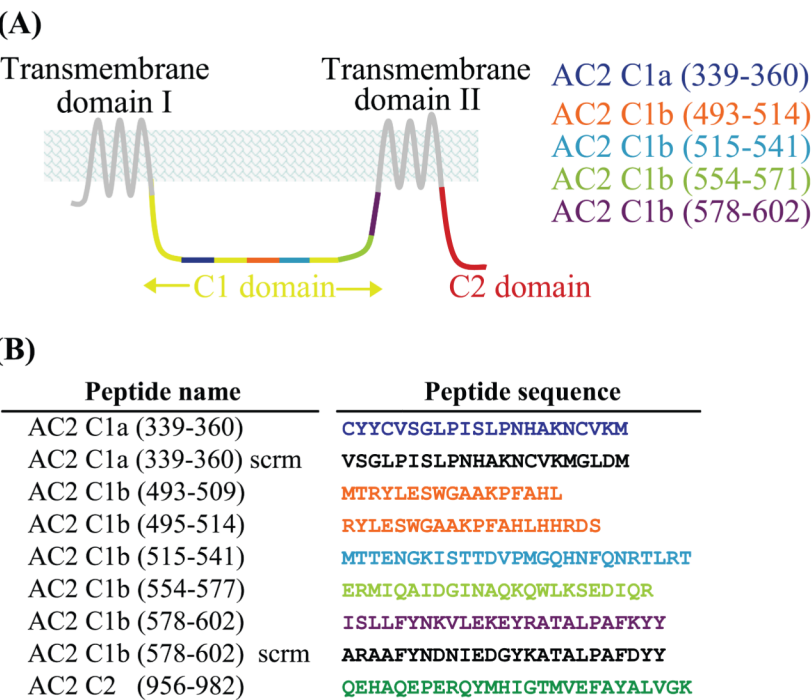


Figure 1. AC2 peptide design
(A) Schematic of the AC2 transmembrane domains and cytosolic (C1 and C2) domains is shown. Transmembrane domains are shown in grey, C1 domain in yellow and C2 domain in red. Peptides are various colors, as indicated by the list on the right. (B) Table summarizing peptide sequences assayed in this study. The sequences are color coded according to the schematic in A and numbered according to the AC2 sequence (Rat; UniProt accession number P26769).

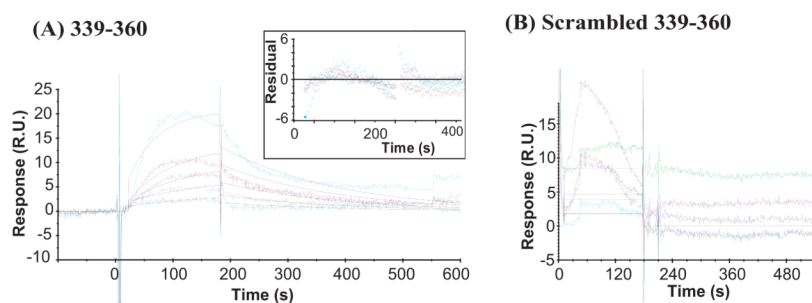


Figure 2. Biacore binding isotherms for interaction between $G\beta\gamma$ and immobilized AC2 C1a peptides and $G\beta\gamma$

Biacore data is shown for binding between $G\beta\gamma$ and (A) the AC2 C1a (339-360) peptide and (B) the scrambled form of the AC2 C1a (339-360) peptide. In order to scramble the 339-360 sequence, several residues were swapped to those with opposite charges and several alanine substitutions were made. The peptides were biotinylated and immobilized and $G\beta\gamma$ was flowed over each chip at 12.5, 25, 50, 100 and 200 nM and at a flow rate of 20 $\mu\text{L}/\text{min}$. The residual is an indication of efficiency of the data fitting to the binding isotherm.

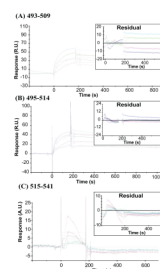


Figure 3. Biacore binding isotherms for interaction between $G\beta\gamma$ and immobilized AC2 C1b PFAHL region peptides

Biacore data is shown for binding between $G\beta\gamma$ and various AC2 C1b PFAHL region peptides: AC2 C1b 493-509 (A), 495-514 (B) and 515-541 (C). The peptides were biotinylated and immobilized and $G\beta\gamma$ was flowed over each chip at 12.5, 25, 50, 100 and 200 nM and at a flow rate of 20 $\mu\text{L}/\text{min}$. The residual is an indication of efficiency of the data fitting the binding isotherm.

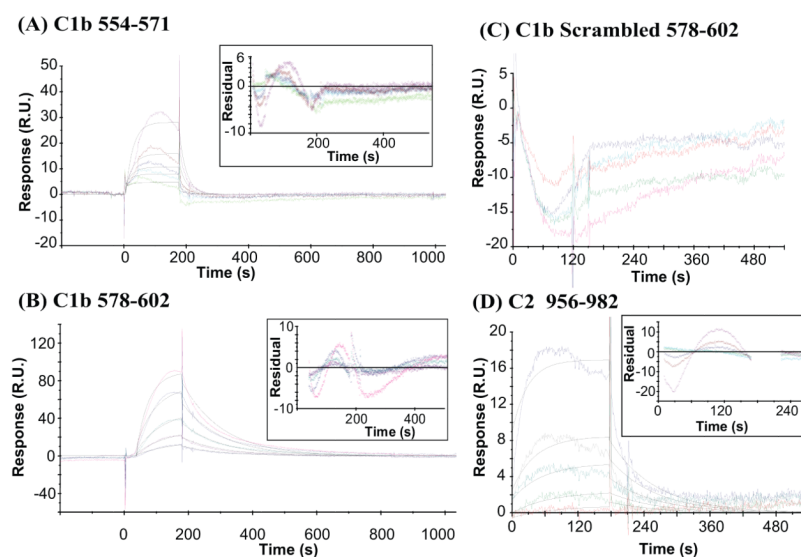


Figure 4. Biacore binding isotherms for interaction between $G\beta\gamma$ and immobilized AC2 C1b and C2 peptides

Biacore data is shown for binding between $G\beta\gamma$ and various AC2 peptides: AC2 C1b 554-571 (A), AC2 C1b 578-602 (B), a scrambled form of the AC2 C1b 578-602 (C) and the QEHA peptide (AC2 C2 956-982) (D). The AC2 C1b 578-602 sequence was scrambled by substituting charged amino acids with amino acids containing the opposite charge. The peptides were biotinylated and immobilized and $G\beta\gamma$ was flowed over each chip at 12.5, 25, 50, 100 and 200 nM and at a flow rate of 20 μ L/min. The residual is an indication of efficiency of the data fitting the binding isotherm.

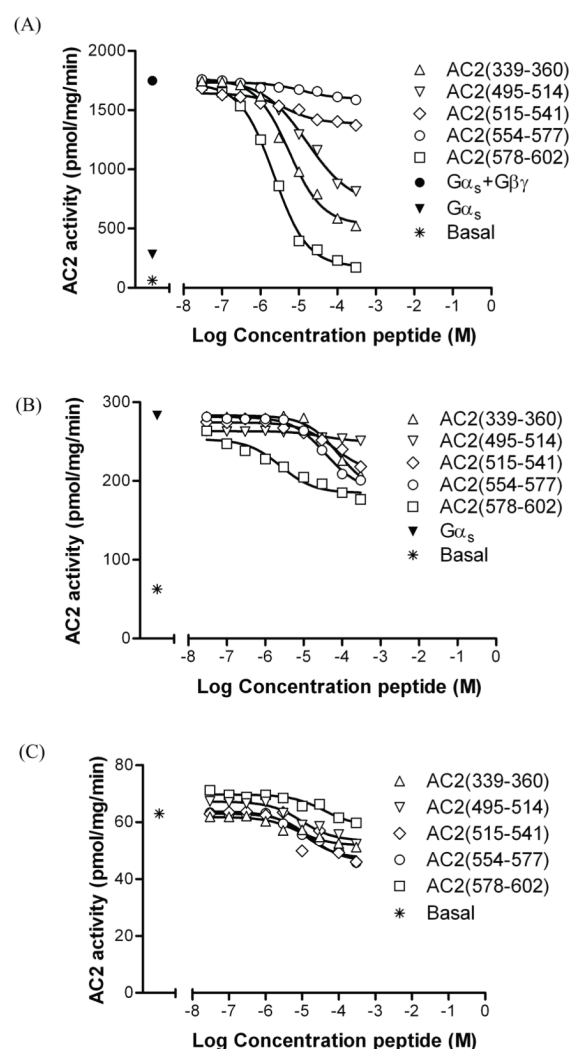


Figure 5. Modulation of AC2 activation by $G\beta\gamma$ by various AC2 peptides

Plots of AC2 activity under various conditions are shown. AC2 activity was measured using a radiometric assay where $[\alpha P^{32}]$ -ATP is converted to $[\alpha P^{32}]$ -cAMP. The activity is expressed in units of pmol of cAMP generated per milligram of membrane protein per minute (pmol/mg/min). (A) AC2 was stimulated with $G\alpha_s$ alone, $G\alpha_s + G\beta\gamma$ or $G\alpha_s + G\beta\gamma$ with increasing concentrations of the C1a or C1b peptides. (B) AC2 was stimulated with $G\alpha_s$ alone or $G\alpha_s$ with increasing concentrations of the C1a or C1b peptides. (C) AC2 basal activity was measured with increasing concentrations of the C1a or C1b peptides. Open symbols represent $G\alpha_s + G\beta\gamma$ + various peptides, \blacktriangledown $G\alpha_s$ alone, \bullet $G\alpha_s + G\beta\gamma$ and $*$ basal.

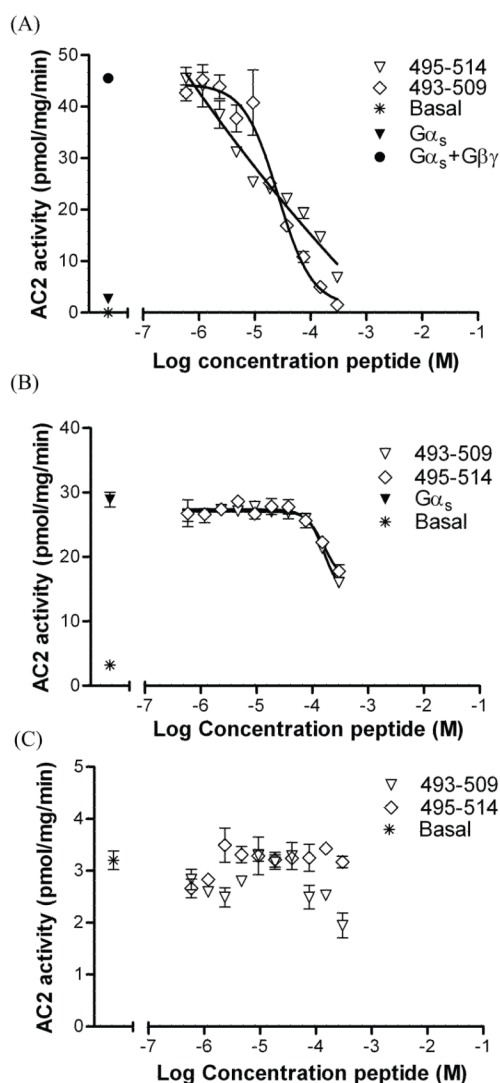


Figure 6. Modulation of AC2 activation by $G\beta\gamma$ by AC2 PFAHL C1b peptides

Plots of the AC2 activity under various conditions are shown. AC2 activity was measured using a commercially available cAMP Lance™ assay kit. The activity is expressed in units of pmol of cAMP generated per milligram of membrane protein per minute (pmol/mg/min). (A) AC2 was stimulated with $G\alpha_s$ alone, $G\alpha_s + G\beta\gamma$ or $G\alpha_s + G\beta\gamma$ with increasing concentrations of the PFAHL C1b peptides. (B) AC2 was stimulated with $G\alpha_s$ alone or $G\alpha_s$ with increasing concentrations of the PFAHL C1b peptides. (C) AC2 basal activity was measured with increasing concentrations of the PFAHL C1b peptides. Open symbols represent $G\alpha_s + G\beta\gamma$ + various peptides, ▼ $G\alpha_s$ alone, ● $G\alpha_s + G\beta\gamma$ and * basal.

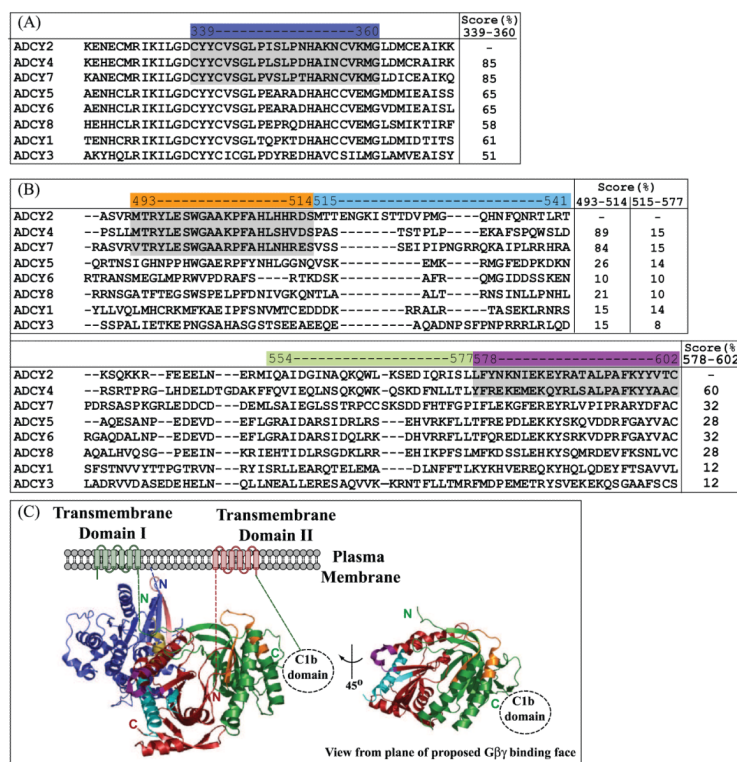


Figure 7. Homology of regions within the C1 and C2 domains of AC isoforms and structural analysis of AC activation

Sequence alignments of a segment from the C1a region of AC2 (A) and the C1b region of AC2 (B). The score represents the percent homology for each region between each AC and AC2 as generated by alignments using EMBL-EBI ClustalW software. Regions of high homology are highlighted in grey and the sequence ranges covered by the AC2 peptides in this study are depicted at the top of the sequence alignments, color coded as in Figure 1. AC rat sequences were used when available otherwise, the AC mouse sequence was used. AC accession numbers and species (accession number/ AC isoform/ species) were as follows: P26769/ ADCY2/ RAT, P26770/ ADCY4/ RAT, P51829/ ADCY7/ MOUSE, Q04400/ ADCY5/ RAT, Q03343/ ADCY6/ RAT, O88444/ ADCY1/ MOUSE, P40146/ ADCY8/ RAT, P21932/ ADCY3/ RAT, and P51830/ ADCY9/ MOUSE. (C) Cartoon rendering of AC- $G\alpha_s$ structure where AC5 C1 is shown in green, AC2 C2 is shown in red and $G\alpha_s$ is shown in blue. The AC2 C2 peptide sequence (QEHA 956-982) is highlighted in cyan, AC2 C2 KF loop (927-933) is highlighted in purple and the AC5 C1a peptide region (339-360) is highlighted in orange. The Switch I region of $G\alpha_s$ is highlighted in pink and the Switch II is in yellow. Dashed lines with the color corresponding to the respective AC region or $G\alpha_s$ region represent linkages to the membrane for which the amino acid sequences have been omitted from the structure. The structural view on the right is rotated approximately 45° with respect to the view on the left and $G\alpha_s$ was omitted for clarity. The protein renderings were made using PyMol [35] and the coordinates from the Protein Data Bank file (accession number 1AZS).

Table 1

Binding constants (K_D) calculated from Biacore plots for the binding of $G\beta\gamma$ to immobilized AC2 peptides. Concentrations of 12.5, 25, 50, 100 and 200 nM of $G\beta\gamma$ were tested for each peptide. The data were fitted with the Biacore Biaevelation software (Version 3.1) and the resulting K_D values are reported for each peptide.

Peptide name (AC2 residue numbers)	K_D (nM)
AC2 C1a (339-360)	40.5 ± 6.3
AC2 C1b (493-509)	2.7 ± 1.3
AC2 C1b (495-514)	4.7 ± 1.7
AC2 C1b (515-541)	>10000
AC2 C1b (554-577)	>10000
AC2 C1b (578-602)	102 ± 14
QEHA C2 (956-982)	13.9 ± 8.8
AC2 C1a (339-360) scrm	---
AC2 C1b (578-602) scrm	---

Percent maximal inhibition values and IC₅₀ values for the activity of each listed peptide to inhibit basal or Gα_s stimulation of AC2 or Gβγ stimulation of Gα_s-stimulated AC2. Peptides were tested at a concentration range of 46 nM to 300 μM. Percent maximal inhibition values were calculated by comparing the cAMP level at 300 μM of each peptide to the respective basal condition. IC₅₀ values were determined from the non-linear regression analysis by GraphPad Prism Version 5.

Table 2

Peptide name (AC2 residue numbers)	Basal		Gα _s -stimulation		Gα _s /Gβγ stimulation	
	% Max Inhibition	IC ₅₀ (μM)	% Max Inhibition	IC ₅₀ (μM)	% Max Inhibition	IC ₅₀ (μM)
AC2 C1a (339-360)	29.2	7.7	36.1	82.3	88.0	5.6
AC2 C1b (495-514)	14.1	>100	15.3	32.9	67.0	13.9
AC2 C1b (515-541)	36.4	11.1	30.9	61.0	27.0	4.5
AC2 C1b (554-577)	36.7	16.7	39.1	36.7	11.5	12.2
AC2 C1b (578-602)	17.4	38.5	50.6	2.5	113.1	2.2